J. Chem. & Cheml. Sci. Vol.2 (1), 61-75 (2012)

Synthesis, Characterization and Catalytic Activity of Ruthenium and Silver Immobilized Heterogeneous Nanoparticle Catalysts

DEVARAJAN EZHILARASU[1] and EAGAMPERAM MURUGAN*

[1]Assistant Professor, Department of Chemistry,
Jei Mathaajee College of Engineering, Kanchipuram,
Siruvakkam, – 631 552, Tamil Nadu, India.
*Department of Physical Chemistry,
School of Chemical Science,
University of Madras, Maraimalai Campus,
Guindy, Chennai – 600 025, Tamil Nadu, India.

ABSTRACT

Intriguing catalytic activity of silver and ruthenium nanoparticles has potential application as a nanostructured catalyst. Metal nanoparticles are of wide interest because of their large surface area and some of the properties which differs them from those of bulk metal solids. The increased catalytic activity of these metal nanoparticles is attributed to their size and shape, which can be controlled be controlled by an insoluble polymer stabilization. The present study is aimed to synthesis, characterize and to determine the catalytic activity of silver and ruthenium nanoparticle immobilized heterogeneous catalysts using insoluble cross-linked (2% and 10%) polymer-supported(4-vinylpyridine) beads as common matrices, in reducing the nitro compounds. All the ruthenium and silver immobilized PS-P4VP beads were catalytically active; irrespective of the type of metal low cross linked polymers were more active. The low cross linked ruthenium immobilized beads were superior and the recycling efficiency these beads were also higher.

Keywords*:* Ruthenium, silver, nanoparticle, polymer matrix, cross linking, catalysts.

1. INTRODUCTION

Metal nanoparticle catalysis has drawn considerable attention due to their intriguing chemical and physical properties and potential applications that results in enhanced catalytic activity and selectivity of nanostructured catalysts [1-3]. The synthesis of

metal nanoparticles of desired size and shape has received enormous importance in nanotechnology because of their characteristic shape and size dependent optical, electronic and chemical properties. The novel properties of these materials have found extensive uses in microelectronics, electronics, magnetic devices, non-linear optics, chemical and biochemical sensors and in catalysis. Metal nanoparticles are of wide interest because of their large surface area and some interesting properties which are different from those of bulk metal solids. Among them, the increased catalytic activity is known to exist in nanoparticles, correlating with their sizes and shapes. The smaller the metal particles are, the larger the fraction of metal atoms exposed on the surface, greater the probability of the reactant molecules have to access to particles. In catalytic applications, a uniform dispersion of nanoparticles and an effective control of particle size are usually expected. The unique features of metal nanoparticles are significantly influenced by such parameters as metal nanoparticle size, organization of the nanoparticle crystal lattice, nanoparticle surface, (amount of defects)[4] and the chemical nature of the microenvironment surrounding the nanoparticle[5]. A great effort has been directed towards preparing metal nanoparticles by many methods such as chemical reduction, UV photolysis, thermal decomposition, metal vapor deposition, electrochemical reduction, sonochemical decomposition, microwave irradiation and the recently reported rapid expansion of supercritical nuid solutions (RESS). To obtain stable mono- and nano-size catalysts, metal nanoparticles are usually dispersed by polymer[6,7] surfactants[8] and inorganic supports. For the solid supported catalysts, the classical impregnation methods offer little control over uniformity and precise control of particle size. In homogeneous catalysis, polymer-protected metal nanoclusters were prepared chemically by reduction of corresponding metal salts in the presence of polymer, and used as catalysts for various reactions[9-11]. The addition of polymer is necessary to control the particle size and prevent inter-particle sintering. However, their application is restricted because of the difficulty in separating catalysts from the reaction mixture for recycling. Also, the catalytic nanoparticles formed on the inorganic support surface or carbon does not allow a precise control over nanoparticle size and morphology[12,13]. In order to overcome these problems, insoluble polymer-stabilized metal nanoparticles have been synthesized with improved stabilization of the particles and the enhanced control over particle characteristics[14-18]. Many methods have been developed to prepare nanoparticles, polymer-anchored metal nanoparticles that can control particle size and prevent them from agglomeration[19, 20]. Among the known nanoparticles, ruthenium (Ru) and silver (Ag) are widely studied because of their characteristic optical, spectroscopic and catalytic properties. They have been widely exploited for use in photography, catalysis, biological labeling, photonics and surface enhanced Raman scattering, among others. It has been observed in most cases, that due to the existence of a highly exposed surface, the nanoparticles tend to aggregate and form large clusters even during the preparative process. The metal catalyzed reduction of

nitro compounds represents a class of reactions widely employed in industrial organic synthesis which are commonly encountered also in large scale chemical production plants. Several reports are available on the reduction of nitro compounds using metal nanoparticles. However only, very few studies have been reported on the reduction of nitro compounds in the presence of insoluble metal NPs. The present study is aimed to synthesis, characterize and to determine the catalytic activity of silver and ruthenium nanoparticle immobilized heterogeneous catalysts using insoluble cross-linked (2% and 10%) polymer-supported(4-vinylpyridine) beads as common matrices, in reducing the nitro compounds.

2. MATERIALS & METHODOLOGY

2.1 Reagents

Styrene (Aldrich), 4-vinylpyridine (Lancaster), divinylbenzene (Lancaster), gelatin (SD fine), boric acid (SRL), poly vinyl alcohol (SRL), sodium hydroxide (SRL), sodium nitrite (SRL), AIBN ruthenium (III) chloride hydrate ($RuCl_3$. nH_2O, Loba), silver nitrate ($AgNO_3$, SRL), ethanol (SRL) and sodium borohydride (SD fine), 4-nitrophenol (Loba), 2-nitroaniline (Loba), sodium borohydride (SD fine) were used as such without any further purification. Deionized water obtained by multiple distillations was used for the preparation of solutions.

2.2 Preparation of insoluble cross-linked polymer-supported Poly (4-vinylpyridine) (PS-P4VP) beads as a common matrix

Insoluble cross-linked polymer-supported poly (4-vinylpyridine) (PS-P4VP) beads was prepared by a method as reported earlier, with the cross-linker monomer ratio as 2% and 10% respectively [21]. This involves suspension co-polymerization of 73% styrene (ST) and 25% 4-vinylpyridine (functional monomer) cross-linked with 2% divinylbenzene (DVB).

Exactly 1.35g of gelatin, 2.55 g boric acid and 2.25 g polyvinyl alcohol were dissolved thoroughly in 30, 60 and 130mL of double distilled hot water (50^{o}C). Then these solutions were mixed together at room temperature. The pH of the solution was adjusted to 10 by adding 25% aqueous sodium hydroxide solution and then 0.1g of sodium nitrite was added to maintain the conformation of gelatin. The solution was then transferred to a 250mL three necked RB flask equipped with an overhead mechanical stirrer and a reflux condenser. Nitrogen was passed continuously and the temperature was maintained at 50^{o}C. After half an hour the organic phase containing 3.3 g of DVB, 58.52 g of styrene, 25.76 g of 4-vinylpyridine and 0.4125 g of AIBN was thoroughly mixed and added to the reaction flask. The blade level of the stirrer was adjusted so that the tips were in organic phase and most of the blade in aqueous phase. The temperature was increased to 70^{o}C and stirrer speed was maintained at 400 rpm using tachometer. The polymerization reaction was allowed 48 hours for completion. The polymer beads were filtered through a Buckner funnel and washed with hot water and cold methanol repeatedly until the wash solution was clear. Then it was dried at 60^{o}C in a vacuum oven for 2 days and the dried beads were sieved into different sizes. Similarly, by fixing the percentage of cross-linking monomer as

10% (instead of 2%) and styrene as 65%, another type of PS-P4VP beads were synthesized (Scheme 1).

2.3 Preparation of Ruthenium Immobilized Heterogeneous Nanoparticle-Polymer Beads (PS-P4VP-RuNps)

The immobilization of RuNPs onto the PS-P4VP polymer matrix was performed using $RuCl_3.H_2O$ as a metal precursor solution. In a 100ml round-bottomed flask, 500 mg of type-I PS-P4VP and type-II PS-P4VP beads (7.5×10^{-3} mol) were taken individually and swelled with 50ml of ethanol, overnight. The polymer beads in the respective flask were purged with nitrogen for 1 hr. After 1 hr, $RuCl_3.H_2O$ (5 mg, 1.5×10^{-4} mol) was added and a dark red solution was formed. The containers containing red mixture were placed in an oil bath with a magnetic stirrer and the temperature was maintained at 80ºC. After ten minutes, the color of the solution changed from red to yellow, then turned green after an hour. Then, 2 equivalents of $NaBH_4$ was added to each flask and then refluxed for 24 hrs and finally the reduced forms of RuNPs immobilized PS-P4VP beads (type-I and type-II) having dark brown color was obtained. The nanoparticle immobilized beads were then filtered through Buchner funnel, washed thrice with ethanol and dried in an oven at 60ºC for 12 hours (Scheme 2).

2.4 Preparation of Silver Immobilized Heterogeneous Nanoparticle-Polymer Beads (PS-P4VP-Ag NPs)

Immobilization of AgNPs onto the PS-P4VP polymer matrix was performed using $AgNO_3$ as a metal precursor solution as the case with RuNP immobilized polymer beads. 500 mg of type-I and type-II PS-P4VP beads (7.5×10^{-3} mol) were taken individually in a 100ml round-bottomed flask and swelled with 50 ml of ethanol, overnight. The respective polymer beads in the flask were purged with nitrogen for 1 hr. After 1 hr, $AgNO_3$ (5 mg, 1.5×10^{-4} mol) was added to each container and thus colorless solution was formed in both the container. Then the solution was stirred and refluxed in an oil bath with a magnetic stirrer at 80ºC. The reaction mixture should be protected from light exposure so as to avoid the photochemical reduction of Ag^+. After ten minutes, the color of the solution was changed into light yellow. Subsequently, the color was changed to dark yellow after 1 hr. Then, 2 equivalents of $NaBH_4$ were added to the respective solution and the containers were refluxed with stirring for 24 hours. The reduced forms of AgNPs immobilized in type-I and type-II PS-P4VP heterogeneous nanoparticle-polymer beads with black color were filtered through Buchner funnel, washed thrice with ethanol and dried in oven at 60ºC for 12 hrs. The color changes were related to the reduction of Ag^{2+} NPs (Scheme 3).

2.5 Comparative Study on the Catalytic Activity of Ruthenium and Silver immobilized PS-P4VP beads for the reduction of 4-NitroPhenol and 2-NitroAniline

The catalytic efficiency of PS-P4VP-RuNPs and PS-P4VP-AgNPs catalysts was examined by the reduction of 4-nitrophenol/2-nitroaniline respectively, under an identical pseudo-first order condition (Scheme 4 & 5).The individual

kinetic experiments was performed, by taking two 10 ml, two necked RB flask to which 5 ml of 4-NP or 2-NA (0.2mM), 5 ml of aqueous $NaBH_4$ (100mM) and 25 mg of 4 different catalysts type-I and type-II PS-P4VP-RuNPs and PS-P4VP-AgNPs catalysts were added individually. The reaction medium was agitated with magnetic stirrer at ambient temperature. The progress of the respective reactions was monitored through UV-Vis spectrophotometer maintaining the wavelength from 200 to 800nm. The respective mixture i.e. 4-NP/2-NA were withdrawn from the reaction medium at every 5 minutes interval and the absorption spectrum was recorded quantitatively against time using UV-Visible Spectrophotometer. The rate constant was calculated using the following formula irrespective of the reaction.

$$k_{obs} = \ln[(A_\infty - A_0)/(A_\infty - A_t)]/t$$

Where A_0-initial absorbance,
A_t-absorbance at time't',
A_∞-absorbance at infinity time.

2.6 Recycling efficiency of type-I PS-P4VP-RuNPs through reduction of 4-NP

The stability of NPs immobilized heterogeneous catalysts is an important factor in the industries. In order to examine this factor, the type-I PS-P4VP-RuNPs catalysts used in the first cycle was filtered and then they were used individually again to conduct the same 4-NP reduction under identical reaction conditions (as followed in their corresponding first cycle).

2.7 UV-Visible Spectrophotometer Analysis

The immobilization of ruthenium and silver nanoparticles on type-I and type-II beads were confirmed from normal micrograph, UV-visible spectrophotometer. UV-Vis spectra of the samples were recorded on Techomp 8500 UV-Vis spectrophotometer with analyst software. The measurements were carried out between the wavelength range of 200 - 800 nm.

2.8 FT-IR measurements

FT-IR spectra of the samples were recorded on Bruker Tensor-27 FT-IR spectrophotometer. Background calibrations have been carried out using pure KBr pellet, and the measurements were carried out between range 400 - 4000 cm^{-1} at 25 ºC.

2.9 Scanning electron microscope (SEM)

The surface morphology of the polymeric beads and nanoparticle immobilized beads were analyzed with the help JEOL JSM-6360 scanning electron microscope (SEM). The polymeric materials are made conducting by platinum coating with the help of JEOL JSM-6360 auto fine-coating ion sputter.

3. RESULT

3.1 Type-I and Type-II Ruthenium Nanoparticle Immobilized Beads

3.1.1 Color Changes

Initially, a dark red solution was obtained by the addition of PS-P4VP beads into the $RuCl_3.H_2O$ and $NaBH_4$ solution. On

refluxing the reaction mixture the color turned yellow and after 3 hrs, it turned green. As the stirring and refluxing continued for 24 hrs, the reaction mixture turned dark brown (Fig. 1a).

3.1.2 UV-Visible Spectrophotometry

In the UV-Visible spectrum, there was a peak at 409nm initially, with the increasing time interval, the height of the peak at 409nm was found to decrease gradually and shifted to a higher frequency in a step by step manner. After 24 hours, the absorption peak disappeared completely which indicates complete reduction of Ru^{3+} to Ru^0 (Fig. 2a).

3.1.3 Fourier Transform-Infra Red (FT-IR) Spectroscopy

In the FT-IR spectra of both type-I and type-II Ruthenium immobilized PS-P4VP catalysts, the peak intensity of C=N stretching at 1597 cm^{-1} was found to be decreased and a new peak appeared at 1745 cm^{-1} and 1747 cm^{-1} respectively (Fig. 4a & 4b) when compared with that of the FT-IR spectrum of PS-P4VP beads (Fig. 3a & 3b).

3.1.4 Scanning Electron Microscope (SEM)

White spots were observed on the surface of the beads (Fig. 6b & 6e) when compared with the corresponding type-I and type-II PS-P4VP matrices (Fig. 6a & 6d).

3.2 Type-I and Type-II Silver Nanoparticle Immobilized Beads

3.2.1 Color Changes

The colorless solution turned yellow upon addition of $NaBH_4$, upon continuous stirring and reflux the solution turned black indicating complete reduction of silver (Fig. 1b).

3.2.2 UV-Visible Spectrophotometry

The successive reduction of silver ions was monitored through UV-Vis spectrophotometry. Initially, the solution gives a peak at 422 nm in UV-visible spectrum. Then the peak height was found to decrease gradually with the increase in time. After 24 hrs, appearance of peak at around 422 nm demonstrated that Ag^+ was totally reduced to Ag^0 (Fig. 2b).

3.2.3 Fourier Transform-Infra Red (FT-IR) Spectroscopy

The FT-IR spectra of type-I and type-II PS-P4VP-AgNPs (Fig. 5a & 5b) were compared with that of PS-P4VP beads (Fig. 3a & 3b).

3.2.4 Scanning Electron Microscope (SEM)

Similarly, in the case of SEM analysis for both the type-I and type-II PS-P4VP-AgNPs (Fig. 6c & 6f), were compared with that of plain polymer beads (Fig. 6a & 6d)

3.3 Catalytic Study for the Reduction of 4-NitroPhenol (4-NP) and 2-NitroAniline (2-NA)

In the UV-Vis Spectrum the characteristic peak (absorbance) for the reduction of 4-NP was observed at 400 nm, which in turn was used for the calculation of $k_{obs.}$ Similarly, in the case of 2-NA the intensity of the absorbance of the characteristic peak was observed at 400 nm

which in turn decreased gradually against the time. Here too, the decreasing trend of characteristic peak was recorded at regular intervals of time (5 minutes) and used the same for the calculation of pseudo-first order rate constant. The rate constants for each reduction reaction was calculated and tabulated in Table 1.

3.4 Recycling efficiency

From the absorbance value, the pseudo-first order rate constants were evaluated. The calculated rate constants are given in Table 2.

4. DISCUSSION

The present study deals with the synthesis and characterization of 4 types of heterogeneous nanoparticle catalyst with two kinds of metal ruthenium and silver as catalytic nanoparticle and 2 kinds of 2% (type-i) and 10% (type-ii) cross-linked bead-shaped polymer-supported poly(4-vinylpyridine)-co-styrene beads (ps-p4vp) as a common solid matrix. The obtained 2 types of ruthenium immobilized ps-p4vp-runps catalysts and 2 types of silver immobilized ps-p4vp-agnps heterogeneous nanoparticle catalysts were characterized through uv-visible spectrophotometry, ft-ir spectroscopy and scanning electron microscopy (sem) techniques. The catalytic efficiency of all the 4 types of catalysts were examined by conducting the comparative study for the reductions of two different reactions viz., reduction of 4-nitrophenol and reduction of 2-nitroaniline under identical pseudo-first order conditions in the presence of $nabh_4$. The ftir spectrum of the ruthenium immobilized ps-pvp indicates that the immobilization of runps is via interactions between the nitrogen of pyridine ring of ps-p4vp beads and ruthenium. This in turn along with the scanning electron microscope results confirms the immobilization of ruthenium nanoparticle catalysts. Disappearance of alcohol o-h stretching at 3400 cm^{-1} and appearance of aldehyde c=o stretching at 1778 cm^{-1} was observed in the ftir spectrum of filtrate which confirms the formation of nanoparticles by complete oxidation of ethanol to acetaldehyde[22]. The density/ number of white dots was found to be higher for type-i ps-p4vp-runps than with type-ii ps-p4vp-runps catalyst. This is due to the increase in the percentage of cross-linking agent (i.e. Dvb) would prevents immobilization of runps, because at high concentration of dvb (10%), the functional group 4-vinylpyridine would have possibly been buried inside the matrices and hence the pyridine nitrogen atoms may not be available freely for binding with ruthenium. Since, most of the functional pyridine moieties are buried inside the matrix; the very low porosity decreases the interaction between metal and pyridine group and resulting in less amount of metal load. But, in the case of type-ii (2% dvb) since the cross-linking agent has lower ratio, more number of pyridine nitrogen atoms should be available without any steric polymeric network and thus more amount of ruthenium ions were bound to the free pyridine moiety, resulting in the immobilization of more number of runps in type-i ps-p4vp-runps and thus reflecting the rich white spots in sem images. In case of silver immobilized beads, the peak intensity of c=n stretching of pyridine ring in ps-p4vp beads at 1597 cm^{-1}

was found to be decreased with the appearance of new peak at 1747 cm^{-1} (fig. 5a) in the case of type-i ps-p4vp-agnps and at 1745 cm^{-1} (fig. 5b) for type-ii (ps4vp)-agnps respectively which confirms the formation of silver immobilized ps-p4vp-beads[23]. The presence of white patches on the surface of both type-i and type-ii ps-p4vp-agnps beads also confirms the presence of silver nanoparticles[24,25]. The immobilization of silver nanoparticles were higher with type-i ps-p4vp-agnpsthan with type-ii ps-p4vp-agnps which is due to the low availability of pyridine nitrogen in the type-ii ps-p4vp-agnps at higher percentage of cross-linking agent.

From the Table 1, it is understood that among the type-I and type-II PS-P4VP-NPs irrespective of metals, the type-I PS-P4VP-NPs are the most active than type-II PS-P4VP-NPs. This is due to the increase in the percentage of cross-linking agent i.e. 10% DVB. The amount of cross-linking agent (DVB) is an important factor for the performance of the polymer-stabilized nanoparticle catalysts. With higher percentage of DVB, irrespective of the type of nanoparticles the resulting nanoparticle catalysts have reduced mobility of nanoparticle moieties, due to sterically crowded PS-P4VP matrix. As a result, the diffusion of NPs/reactants into the matrices was reduced, resulting in reduced catalytic activity. Therefore, in the catalysis, the observed rate constants were found to decrease for type-II PS-P4VP-NPs catalyst in both the reduction reactions irrespective of metals. Whereas, in the case of 2% PS-P4VP beads, the amount of NPs irrespective of metals increased effectively and thus found to have effective catalytic activity than the type-I catalyst irrespective of metals.

Further, between the type-I PS-P4VP-RuNPs and type-I PS-P4VP-AgNPs, the type-I PS-P4VP-RuNPs was found to be more efficient in terms of rate constant (Table 9). That is, though the molar ratio of polymer matrices to metal is same for both RuNPs and AgNPs, the catalytic activity of RuNPs was higher than that of AgNPs [26-33]. This vast difference may be attributed to the many reasons. However, in the present study, the reasons for increased k_{obs} noticed in type-I PS-P4VP-RuNPs catalyst might be due to (i) relatively fine size distribution and very small size (Fig. 6b) when compared with AgNPs (Fig. 6c) which inturn contributes to the large surface contact area (or) surface-volume-ratio in PS-P4VP-RuNPs, (ii) low potential difference between RuNPs and 4-NP/2-NA than AgNPs and 4-NP/2-NA, with an appreciable change in the Fermi level (iii) the passivation of RuNPs metal surface and (iv) the inherent electronic behaviour of ruthenium metal.

Similarly, the k_{obs} for the recovered (or) first cycle type-I PS-P4VP-RuNPs catalyst in catalyzing the reduction of 4-NP is found to be almost similar on compared with its corresponding original heterogeneous nanoparticle catalyst. This observation directly indicates that the stability of the type-I PS-P4VP-RuNPs catalyst was maintained without any loss (or) leaching of catalytic RuNPs material. Further, the comparative k_{obs} study for 4-NP and 2-NA irrespective of catalyst suggests that the catalysis of 2-NA reduction was found to be more active than with the 4-NP substrate. The increased activity observed in 2-NA may be due to existence of lower

redox potential difference between donor (RuNPs) and receptor (2-NA) on compared with RuNPs versus 4-NP and thus easy acceleration of reduction reaction in 4-NP substrate. These explanations holds good for AgNPs versus 4-NP and AgNPs versus 2-NA system also. The recycling efficiency of superior type catalyst type-I PS-P4VP-RuNPs was found to be stable even after 4imes without any appreciable change in the rate constant.

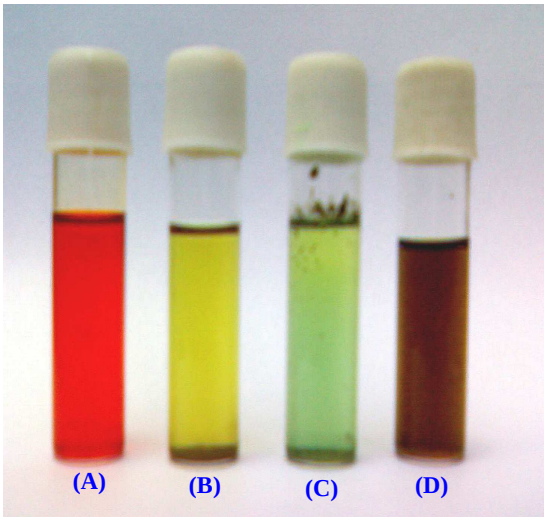

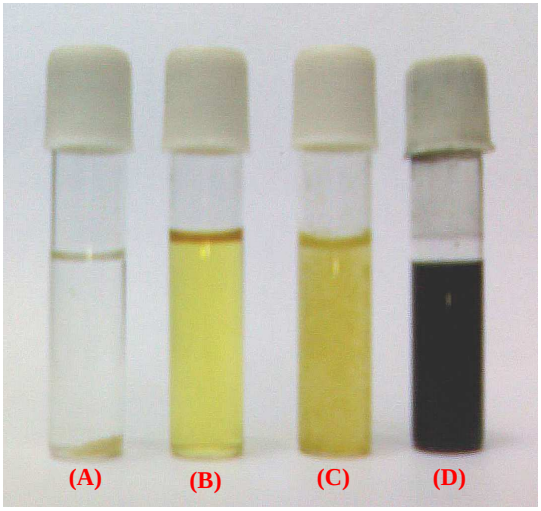

Figure 1: Colour Changes during Nanoparticle Formation

(A) Dark red - Ru^{3+} (B) Yellow - Ru^{2+}
(C) Green - Ru^{1+} (D) Brown - Ru^{0}
a.) PS-P4VP RuNP formation

(A) Colourless – Ag^{2+} (B) Yellow-Ag^{1+}
(C) Dark yellow - Ag^{1+} (D) Black - Ag^{0}
b.) PS-P4VP AgNP formation

Table 1: Comparative catalytic study using new PS-P4VP stabilized NPs Reduction of 4-nitrophenol and 2-nitroaniline

Name of the Catalyst	$k_{obs}\times10^{4}$, sec^{-1}	
	Reduction of 4-nitrophenol	Reduction of 2-nitroaniline
Type-I PS-P4VP-RuNPs	6.76	12.77
Type-I PS-P4VP-AgNPs	4.03	7.95
Type-II PS-P4VP-RuNPs	1.05	3.06
Type-II PS-P4VP-AgNPs	1.02	4.58

Table 2: Recycling efficiency of type-I PS-P4VP-RuNPs through Reduction of 4-Nitrophenol

Number of cycle	$k_{obs}\times10^{4}$, s^{1}
First cycle	4.4094
Second cycle	4.0579
Third cycle	3.9225
Fourth cycle	3.8211

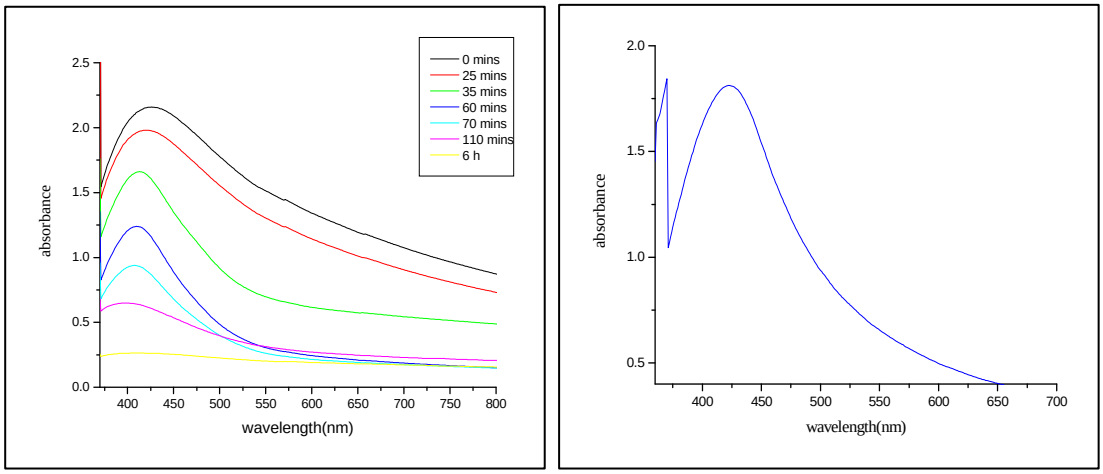

a). PS-P4VP-RuNPs **b). PS-P4VP-AgNPs**

Figure 2: UV-Visible absorption spectrum of Nanoparticle formation on Polymeric surface

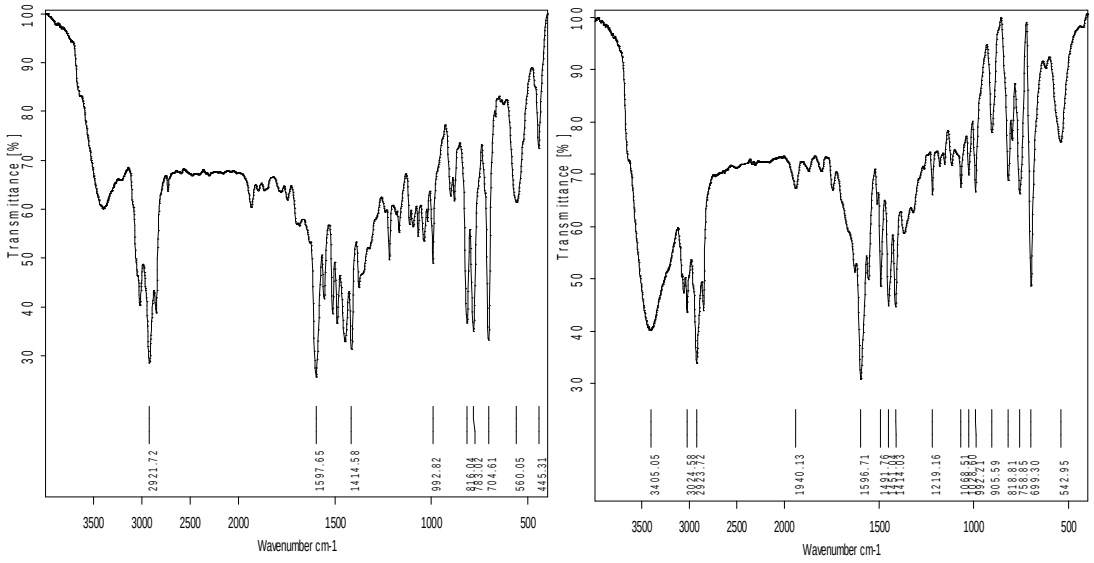

a). Type I PS-P4VP beads **b). Type II PS-P4VP beads**

Figure 3: FT-IR spectrum of Type-I & Type II PS-P4VP beads

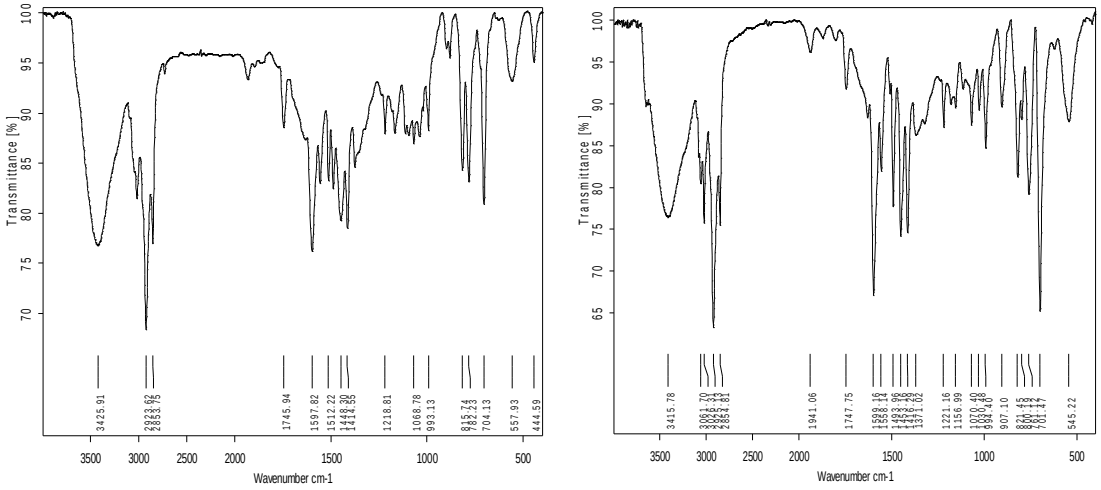

a). Type I PS- P4VP RuNP **b). Type II PS-P4VP RuNP**

Figure 4: FT-IR spectrum of Ru immobilized PS-P4VP

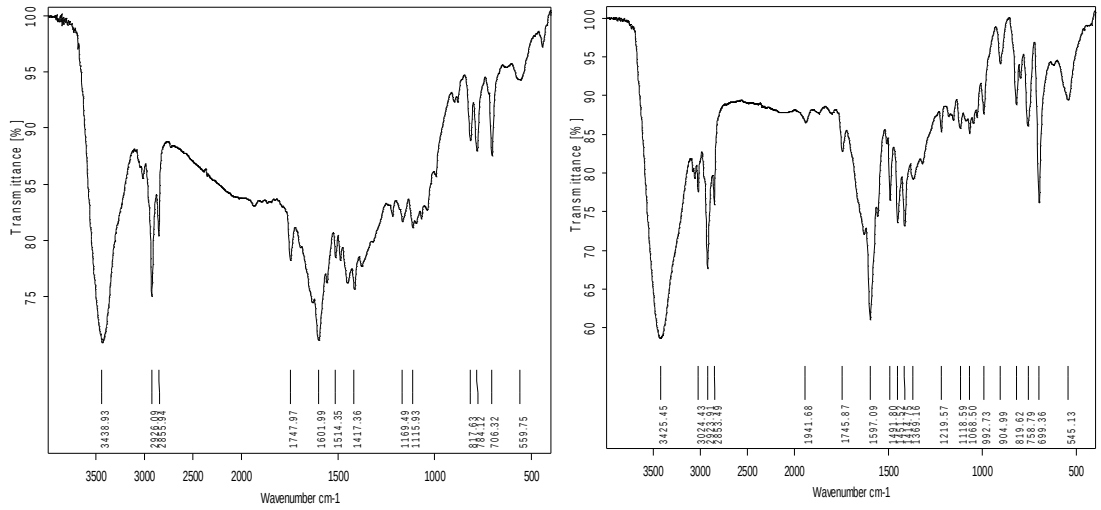

a). Type I PS- P4VP AgNP **b). Type II PS-P4VP Ag**

Figure 5: FT-IR spectrum of Ag immobilized PS-P4VP

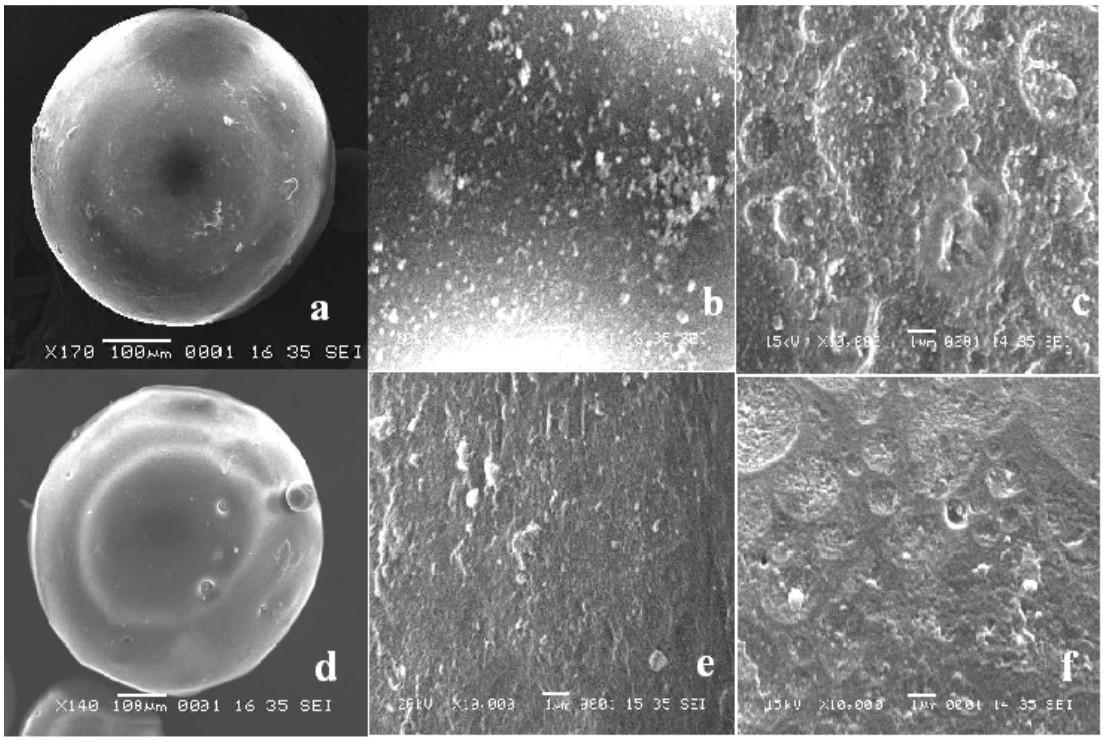

Figure 6: SEM image

a. Type-I PS-P4VP beads, **b. Type-I PS-P4VP- RuNPs beads,**
c. Type-I PS-P4VP-AgNPs beads, **d. Type-II PS-P4VP beads, e. Type-II PS-P4VP- RuNPs beads, f. Type-II PS-P4VP-AgNPs beads.**

Scheme 1

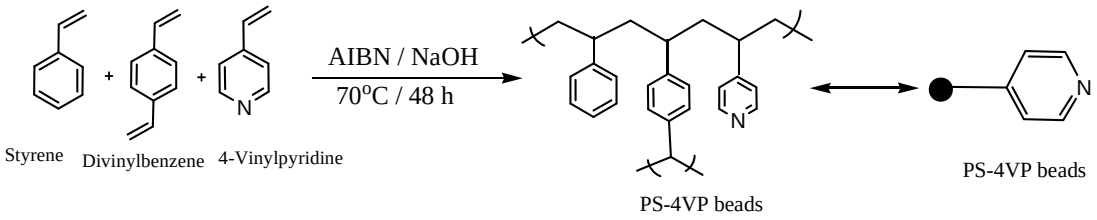

Scheme 2

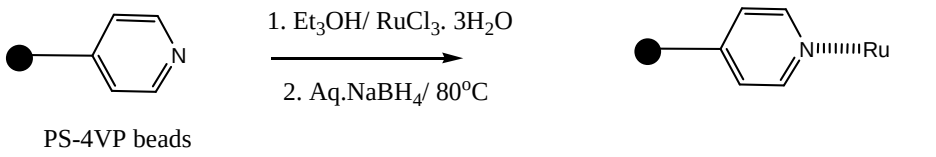

PS-4VP beads

Type-I PS-P4VP-$RuNP_S$ beads

Type-II PS-P4VP-$RuNP_S$ beads

Scheme 3

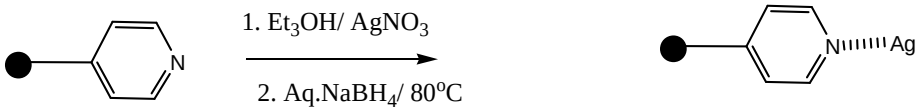

PS-4VP beads

Type-I PS-P4VP-$AgNP_S$ beads

Type-II PS-P4VP-$AgNP_S$ beads

Scheme 4

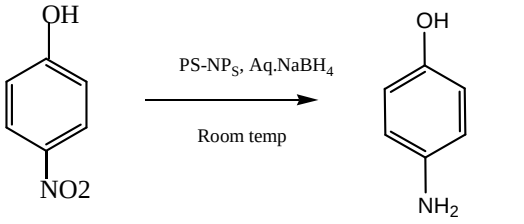

4-Nitrophenol

4-Aminophenol

Scheme 5

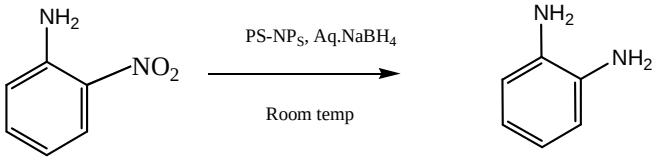

2- Nitroaniline

2-Aminoaniline

CONCLUSION

Metal nanoparticles are of practical interest due to their unique physical properties, chemical reactivity, and potential applications in catalysis. Despite other nanoparticles, ruthenium is unique because of its catalytic activity in synthesis and redox processes. All the four types of Ru and Ag immobilized PS–PVP beads are catalytically active. Type I ruthenium immobilized PS-PVP beads are superior to all the other beads in reducing 4-NP/NA. Continuing efforts in increasing the amount of ruthenium immobilization on to the polymeric beads would help to enhance its recycling efficiency and catalytic activity further.

REFERENCES

1. Brayner, R.; Viau, G.; Verduraz, F.B. *J. Mol. Catal. A.* 227, 182 (2002).
2. Liu, C.; Xu, Y.; Liao S.; Yu, D. *J. Mol. Catal. A.* 253, 157 (2000).
3. Drelinkiewicz, A.; Hasik, M.; Kloc, M. J. *Catal*. 186, 123-133 (1999).
4. Veisz, B.; Kiraly, Z.; Toth, L.; Pecz, B. *Chem. Mater* 14, 2882-2888 (2002).
5. Kralik, M.; Biffis, A. *J. Mol. Catal. A* 177, 113-138 (2001).
6. Kan, C.; Cai, W.; Li, C.; Zhang, L. *J. Mater. Res.* 20, 320-324 (2005).
7. Lee, J.Y.; Yang, J.; Deivaraj, T.C; Too, H. *J. Colloid Interface Sci.* 268, 77- 80 (2003).
8. Pan, C.; Pelzer, K.; Philippot, K.; Chaudret, B.; Dassenoy, F.; Lecante, P.; Casanove, M.J. *J. Am. Chem. Soc.* 123, 7584-7593 (2001).
9. Viau, G.; Brayner, R.; Poul, L.; Chakroune, N.; Lacaze, E.; Vincent, F.F.; Fievet, F. *Chem Mater*. 15, 486-494 (2003).
10. Chakroune, N.; Viau, G.; Ammar, S.; Poul, L.; Veautier, D.; Chehimi, M.M.; Mangeney, C.; Villain, F.; Fiévet, F. *Langmuir*. 21, 6788-6796 (2005).
11. Prabhuram, J.; Wang, X.; Hui, C.L.; Hsing, I.M. *J. phys.Chem. B.* 107, 11057-11064 (2003).
12. Horvath, A.; Beck, A.; Sarkany, A.; Guczi, L. *Solid State Ionics.* 148, 219−225 (2002).
13. Bensebaa, F.; Patrito, N.; Le Page, Y.; L'Ecuyer, L.; Wang, D.S. *J. Mater. Chem.* 14, 3378-3384 (2004).
14. Kralik, M.; Jorık, V.; Kratky, V. *unpublished results.* (2001).
15. Lin, T.B.; Chung, D.L.; Chang, J.R. *Ind. Eng. Chem. Res.* 38, 1271-1276 (1999).
16. Biffis, A.; Landes, H.; Jerabek, K.; Corain, B. *J. Mol. Catal. A.* 151, 283-288 (2000).
17. Kljuev, M.V.; Nasibulin, A.A.; *Kinet. Katal*. 37, 231-233(1996).
18. Biffis, A.; Corain, B.; Cvengrosova, Z.; Hronec, M.; Jerabek, K.; Kralik,M. *Appl. Catal. A.* 124, 355-365 (1995).
19. Shatabdi, P.; Shashi, S.; Sree Harsha, S.; Rao, D.N.; Radhakrishan, T.P. *Chem. Mater.* 17, 9-12 (2005).
20. Van Heerbeek, R.; Kamer, P.C.J.; Leeuwen, P.V.; Reek, J.N.H. *Chem. Rev.* 102, 3717-3756 (2002).
21. Dell'Amico, D.B.; Lora, S.; D'Archivio, A.A.; Galantini, L.; Biffis,A.; Corain, B. *J. Mol. Catal. A.* 157, 173-181 (2000).
22. Kan, C.; Cai, W.; Li, C.; Zhang, L. *J. Mater. Res.* 20,320-324 (2005).
23. Lu, J.Q.; Yi, S.S. *Langmuir.* 22, 3951-3955 (2006).
24. Jana, S.; Pande, S.; Panigrahi, S,; Praharaj, S.; Basu, S.; Pal, S.; Pal, T. *Langmuir*. 22, 7091 -7095 (2003).

25. Jana, N.R.; Gearhert, L.; Murphy, C.*J. Chem. Commun.* 56, 617-678 (2001).
26. Pal, T.J. *Chem. Edu.* 71, 679 (1994).
27. Pal, T.; Sau, T.; Jana, N.R. *Langmuir*. 13, 1481-1485(1997).
28. Henglein, A. *Chem. Rev*. 89, 1861-1873 (1989).
29. Pradhan, N. *Colloids and Surfaces A: Physicochem. Eng. Aspects*. 196, 247–257 (2002).
30. Jana, S. *Applied Catalysis A: General*. 313, 41–48 (2006).
31. Zhou, Q. *Thin solid films*. 516, 953-956 (2008).
32. Huang, J.; Jiang, T.; Gao, H.; Han, B.L.Z.; Chang, W.Y.W.; Angew, Z.G. *Chem., Int. Ed.* 43, 1397–1399 (2004).
33. Song, G.X.; Angew, Z. *Chem. Int. Ed.* 45, 266–269 (2006).